Non-Hermitian Quantum Mechanics for High-Order Harmonic Generation Spectra†

Nimrod Moiseyev*,‡ and Manfred Lein§

Department of Chemistry and Minerva Center for Non-Linear Physics, Technion−Israel Institute of Technology, Haifa 32000, Israel, and Max Planck Institute for the Physics of Complex Systems, Nöthnitzer Straβe 38, D-01187 Dresden, Germany

Received: February 14, 2003; In Final Form: April 28, 2003

High-order harmonic generation spectra of atoms and molecules in intense laser fields show a wide plateau of *odd* harmonics, with photon energies high up to the soft X-ray regime. The mechanism leading to the absence of other frequencies, so-called hyper-Raman lines or sidebands, is still unclear. By the use of non-Hermitian quantum mechanics for the many-electron atomic/molecular Hamiltonian system, we derive closed-form expressions for the high-order harmonic generation spectra. The analysis of these expressions provides the (already known) conditions for which the hyper-Raman lines are missing and also the conditions for which they are observable. The new information obtained here is proof that in order to observe sidebands it is not sufficient to populate two different Floquet states. When the duration of the laser pulse is sufficiently long, the two resonance Floquet states should have similar widths (inverse lifetimes). For short pulses, the condition for observable sidebands is more complicated, and it does not depend directly on the lifetime of the resonance states. By numerical integration of the conventional time-dependent Schrödinger equation, we provide illustrative examples that confirm our conclusions. Our results can be used to design new experiments that will show the fingerprints of the hyper-Raman lines.

1. Introduction

Since L'Huillier et al. have shown in a series of experiments that atoms of a low-pressure gas exposed to an intense laser pulse diffuse electromagnetic radiation consisting of odd harmonics,[1] many more experiments have been carried out.[2] Recently, it has been shown that high-order harmonic generation (HG) spectra can be controlled through the shape and the phase of the laser pulse.[3] In this experiment, the dominant high harmonic was in the soft X-ray regime. Therefore, atoms driven by linearly polarized light can perhaps be used as a source of coherent X-ray radiation. Theoretical calculations show that carbon nanotubes driven by circularly polarized light may also be used as a source of coherent X-rays.[4]

The HG process can be understood such that the system first absorbs N laser photons of frequency ω and then emits the absorbed energy in the form of one high-energy photon with frequency $\Omega = N\omega$. An unanswered question, however, is the absence of hyper-Raman lines (so-called sidebands) in the HG spectra. These lines are expected to be emitted in a process where the emission of the high-energy photon leads to a final state that is different from the initial state. The frequency of the emitted photon would then be $\Omega = N\omega - \Delta E/\hbar$ where ΔE is the energy difference between final and initial states. Several explanations have been proposed for the failure to detect the hyper-Raman lines (ref 5 and references therein). Di Piazza and Fiordilino have shown for a one-electron, 1D model Hamiltonian that the hyper-Raman lines have not been observed because they are emitted during a short time interval and therefore are small when compared with harmonic lines that are instead emitted during the entire laser pulse.[5] There is no general explanation, however, for the difficulty in observing the hyper-Raman lines for real many-electron systems where the electron correlations are taken into consideration.

Part of the mechanism that may lead to the generation of sidebands is known. A decade ago, Bavli and Metiu proved that shifted even harmonics might be generated if two Floquet quasi-energy (QE) states with different parity are populated by the laser pulse.[6] The fact that no sidebands have been observed in the experimental HG spectra, even when short pulses were used and therefore most probably different QE states were populated, suggests the following question: Is the Bavli−Metiu condition for sidebands in the HG spectra a necessary condition but not a sufficient one? If the answer to this question is yes, then the next question is naturally, What are the sufficient conditions under which the sidebands in the HG spectra may be observed? If the answer to the first question is no (i.e., if the Bavli−Metui condition is a sufficient one) one should (a) show that the absence of sidebands in the HG spectra is indeed due to the lack of a proper phase-matching condition in the experiment (i.e., due to destructive interference of the radiation emitted from different atoms in the "cloud" of atoms that are embedded in the focus of the laser beam) and (b) determine the maximum number of atoms that can be exposed to the laser pulse without destroying the sidebands.

Our explanation is based on a general derivation of the probability of emission of high-energy photons for arbitrary many-electron atomic/molecular systems. Note that in this paper the harmonic generation of molecules is discussed within the framework of the Born−Oppenheimer approximation. The nonadiabatic effects on the HG spectra are not discussed here, although the equations we derive for the HG spectra also hold for the most general molecular case.

Because the use of non-Hermitian quantum mechanics is a crucial point in our derivation, we first wish to explain the

† Part of the special issue "Donald J. Kouri Festschrift".

* Corresponding author. E-mail: nimrod@tx.technion.ac.il.
‡ Technion−Israel Institute of Technology.
§ Max Planck Institute for the Physics of Complex Systems.

10.1021/jp034390y CCC: $25.00
Published on Web 06/10/2003

motivation and the need to use non-Hermitian quantum mechanics. In conventional (i.e., Hermitian) quantum mechanics, a resonance is associated with a wave packet.[7] In non-Hermitian quantum mechanics, however, each one of the resonances is associated with a single square-integrable QE eigenstate of the complex-scaled Floquet operator.[8,9] The resonance eigenstates can be counted by their nodes and are eigenstates of the symmetry operators that commute with the complex-scaled Floquet operator. On the basis of dynamical symmetry analysis, it has been proven that when the photoinduced dynamics is controlled by a single resonance QE state

(1) The atomic HG spectra consist of odd harmonics only when a linearly or elliptically polarized cw laser is used.[10,11] No high-order harmonics are obtained when a circularly polarized cw laser is applied.

(2) The HG spectra of fixed-in-space molecules consist only of odd harmonics if the molecules are inversion symmetric. Oriented asymmetric molecules also emit even-order harmonics.[12,13] In the case of the HD molecule, for example, this happens as a consequence of dynamics beyond the Born−Oppenheimer approximation, yet in the plateau region of the spectra, the even-order harmonics in HD are smaller than the odd harmonics by more than an order of magnitude.[13]

(3) The molecular HG spectra have different selection rules when a circularly polarized laser beam is used.[11] For example, it was shown that when carbon nanotubes are exposed to circularly polarized light the energy of the first high harmonic can be in the X-ray regime.[4]

Here, by the use of non-Hermitian quantum mechanics, we derive novel closed-form expressions for the HG spectra when the system is initially prepared in a linear combination of several QE resonance states. The analysis of the expressions obtained within non-Hermitian quantum mechanics shows that the Bavli−Metiu conditions for the generation of even-order and shifted even/odd-order harmonics (i.e., sidebands) have to be extended by another crucial condition: the two interfering resonance Floquet QE states should have similar lifetimes unless ultrashort pulses are used. Using conventional (i.e., Hermitian) quantum mechanics, it is difficult to compare in a precise way the height of the peaks in the HG spectra. Non-Hermitian quantum mechanics enables us to associate the height of the peaks with the lifetimes of the resonance Floquet QE states that control the photoinduced dynamics.

In this paper, we will show how the approach via non-Hermitian quantum mechanics leads to the following conclusions:

(a) There are different series of hyper-Raman lines. Each one of the hyper-Raman series is an even or odd harmonic spectrum that is shifted by the difference between the energies of two resonance metastable QE states that are populated during the time when the laser is turned on. The shifted even-order harmonics are obtained when the two QE resonance states have different parity (i.e., they are nondegenerate eigenstates of the dynamical symmetry operator). These results are in complete agreement with those obtained by the use of the conventional quantum mechanics.[6]

(b) The dominant hyper-Raman spectrum results from the interference between long-lived QE resonance states that are populated during the time when the laser pulse is switched on. The hyper-Raman lines show up when two QE states with similar lifetimes are populated. If the lifetimes of the populated QE states are very different, then the hyper-Raman lines are small compared to the odd harmonics generated by the longest-lived QE state unless ultrashort pulses are used.

Non-Hermitian quantum mechanics enables us to find the conditions under which sidebands appear in the spectra. Of course, Hermitian and non-Hermitian quantum mechanics are physically equivalent and should lead to the same results. Our results should therefore be confirmed by carrying out simulations within conventional (Hermitian) quantum mechanics. To that end, we have also studied illustrative numerical examples within the framework of Hermitian quantum mechanics. The numerical results are obtained by integrating the conventional time-dependent Schrödinger equation. They fully confirm our conclusions about the conditions under which hyper-Raman lines are generated.

Because in the experiments the dominant QE state is usually the longest-lived resonance state, which is associated with the field-free ground state, it is very hard to observe hyper-Raman lines in the measured spectra. Using the same optimal control technique used by Bartels and co-workers in their experiments[3] or by using the stimulated Raman adiabatic passage (STIRAP) scheme,[14] one can design a laser pulse such that two QE resonance states are populated. These can have very different energies, but if they have similar widths, hyper-Raman lines should be observed.

2. Floquet Theory of Harmonic Generation

In this section, we give a brief introduction to the application of Floquet theory[15] to harmonic generation (see also ref 6 for a previous discussion). Let us consider the case of a laser pulse with a turn-on time of less than 20 optical cycles and a subsequent constant profile of more than 20−50 cycles. An optical cycle is equal to $T = 2\pi/\omega$ where ω is the laser frequency. If the photoinduced dynamics is controlled by a single Floquet QE state, then we can use the single-Floquet-state approximation[16,17] where we do not take into consideration the possible appearance of hyper-Raman lines in the high-order harmonic generation spectra. In this paper, we consider the case where during the time when the laser pulse is switched on several QE states are populated. As the laser-pulse profile becomes stable, the system is described by a wave packet given by

$$|\Psi_0(t=0)\rangle = \sum_k C_k |\Phi_k(t=0)\rangle \tag{1}$$

where $t = 0$ is a reference time when the laser-pulse envelope reaches its maximum value F_0. We assume that no relevant high harmonics are produced during the turn-on time. This approximation becomes exact for the highest harmonics because it follows from the derivation of the HG cutoff law[18] that the highest frequencies are generated only at the peak intensity.

For the sake of simplicity and without loss of generality, we use here box quantization. The continuum spectrum is discrete and becomes denser as the box size is increased. As we will discuss later, the use of box quantization plays an important role in our derivation of time-independent expressions for the probability of observing high-order harmonics.

The time-periodic QE states $|\Phi_k(t)\rangle = |\Phi_k(t + nT)\rangle$ are eigenstates of the Floquet operator $\hat{\mathscr{H}}_F$, which has a continuous energy spectrum (quasi-continuous because of the use of box quantization),

$$\hat{\mathscr{H}}_F|\Phi_k(t)\rangle = E_k|\Phi_k(t)\rangle \tag{2}$$

where

$$\hat{\mathscr{H}}_F = -i\hbar \frac{\partial}{\partial t} + \hat{\mathscr{H}}_0 + eF_0 \sum_j \hat{z}_j \cos(\omega t) \tag{3}$$

Here, $\hat{\mathscr{H}}_0$ is the many-electron 3D Hamiltonian of the field-free atom/molecule. The dipole operator $eF_0\hat{z}_j$ acts on the jth electron of the atom/molecule. The quasi-energy E_k is defined modulo $\hbar\omega$ (i.e., $E_k + N\hbar\omega$ with an integer N is also an eigenvalue of the Floquet operator). The electric field points along the z direction, and the laser propagates along a line in the xy plane. The interaction with the laser is treated in the dipole approximation. The power spectrum emitted by the atom/molecule is obtained by taking the Fourier transform of the electron acceleration $a(t)$[19]

$$a(t) = \frac{d^2}{dt^2}\langle \Psi_0(t)|\sum_j \hat{z}_j|\Psi_0(t)\rangle \tag{4}$$

where the time-dependent many-electron state $|\Psi_0(t)\rangle$ is given by

$$|\Psi_0(t)\rangle = \sum_k C_k \exp(-iE_k t/\hbar)|\Phi_k(t)\rangle \tag{5}$$

The Fourier components of $|\Phi_k(t)\rangle$ are time-independent many-electron wave functions (i.e., $|\Phi_k(t)\rangle = \sum_{n=-\infty}^{+\infty} \exp(i\omega nt)|\phi_{n,k}\rangle$). Because the field-free potential is real, $\{|\phi_{n,k}\rangle\}$ can be taken as real functions of the electronic coordinates, even when the spectrum is degenerate. By substituting eq 5 into eq 4, one finds that the emitted power spectrum is given by

$$\begin{aligned}\sigma(\Omega) &= \left|\int_0^\infty dt \exp(-i\Omega t)\, a(t)\right|^2 \\ &= \left|\lim_{\epsilon\to 0+} \sum_{k',k} C_{k'}^* C_k \right. \\ &\quad \times \sum_{n=-\infty}^{+\infty} \sum_{n'=-\infty}^{+\infty} \\ &\quad \left. \frac{((E_k - E_{k'})/\hbar + \omega(n'-n))^2}{\Omega - [(E_k - E_{k'})/\hbar + \omega(n'-n)] + i\epsilon} \langle \phi_{n',k'}\left|\sum_j \hat{z}_j\right|\phi_{n,k}\rangle \right|^2 \end{aligned} \tag{6}$$

The time integration in eq 6 starts from $t = 0$ on the basis of the assumption that no relevant harmonics are emitted before the laser profile becomes stable. The equation can be simplified by using the dynamical symmetry properties of the Floquet operator. The dynamical symmetry of the Floquet operator $\{\mathbf{r}_j \to -\mathbf{r}_j;\ t \to t + T/2\}$ holds for atoms and for inversion-symmetric molecules. For example, it does not hold for oriented heteronuclear diatomics. Because of the dynamical symmetry of the Floquet operator, whenever it applies, the Fourier components of the QE Floquet state obey the rule $\phi_{n,k}(\mathbf{r}) = \pm(-1)^n \phi_{n,k}(-\mathbf{r})$.[11] There are two possibilities:

(a) When the quantum numbers n are odd then the Fourier components $\phi_{n,k}(\mathbf{r})$ are odd functions, whereas for even values of n the Fourier components are even functions. The QE states associated with this possibility are members of QE group 1.

(b) When the quantum numbers n are even, then the Fourier components are odd functions, whereas for odd values of n the Fourier components are even functions. The QE states associated with the second possibility are members of QE group 2.

When $k = k'$, then regardless of the group to which the QE resonances belong, $\langle \phi_{n',k}|\sum_j \hat{z}_j|\phi_{n,k}\rangle \neq 0$ only if $n - n'$ is an odd number. This is proof that atoms (and homonuclear diatomic molecules) in monochromatic laser fields and within the framework of the dipole approximation emit only odd-order harmonics when only one QE state is populated. When $k' \neq k$, we should distinguish between two options. One option is that the QE states $|\Phi_k\rangle$, $|\Phi_{k'}\rangle$ belong to the same symmetry group. In such a case, $\langle \phi_{n',k'}|\sum_j \hat{z}_j|\phi_{n,k}\rangle \neq 0$ only if $n - n'$ is odd. However, the corresponding lines in the HG spectra are shifted with respect to the lines obtained when only one QE state controls the dynamics. The second option is that $|\Phi_k\rangle$ and $|\Phi_{k'}\rangle$ belong to different symmetry groups. Then, the dipole transition integrals do not vanish for even values of $n - n'$. In this case, the hyper-Raman lines would be even-order harmonics shifted by the difference between the energy positions of the two considered QE resonance states. Here we have shown that if indeed the poles in eq 6 control the emission spectra then the terms $k = k'$ in eq 6 provide the probability of generating odd high-order harmonics at $\Omega = \omega(2m + 1)$ where $m = 0, 1,..,$ whereas the terms $k \neq k'$ provide the probability of obtaining the hyper-Raman lines in the emission spectra.

3. Harmonic Generation Spectra in Non-Hermitian Quantum Mechanics

Previous work on HG within the framework of non-Hermitian quantum mechanics[16,17] did not take into account the interference between different Floquet states. In this section, we give a brief description of the non-Hermitian approach, and in particular, we discuss a modification of the inner product, which is necessary to obtain the correct physical results for the case of several Floquet states.

Using conventional quantum mechanics requires an integration over continuum states, and the convergence of the box-quantization series expansion of $\sigma(\Omega)$ must be studied carefully. In non-Hermitian quantum mechanics, the electron coordinates $\{x_j, y_j, z_j\}$ are replaced by $\{\exp(i\theta)x_j, \exp(i\theta)y_j, \exp(i\theta)z_j\}$. The quasi-energies become complex, and we obtain resonance QE states $|\Phi_{k_{res}}\rangle$ with quasi-energies

$$E_{k_{res}} = \mathscr{E}_{k_{res}} - \frac{i}{2}\Gamma_{k_{res}} \tag{7}$$

such that $\mathscr{E}_{k_{res}}$ is defined modulo $\hbar\omega$ and $\Gamma_{k_{res}}$ is the resonance width (i.e., the decay rate of photoionization when the dynamics is controlled by a single resonance state).

Then, the integration over energy (or the summation over the discretized continuum energy terms) is replaced by the summation over the resonance poles of the Floquet operator, which upon complex scaling are associated with square-integrable nodal functions. The interference effects with the rotated continuum states can be neglected because the photo-induced dynamics is dominated by the narrow QE resonances. This possibility of distinguishing between resonances and "white" continuum states does not exist in the conventional (Hermitian) quantum mechanics. Unlike the situation in non-Hermitian quantum mechanics, in conventional quantum mechanics, a resonance state is not associated with a single eigenstate of the Hamiltonian, so we cannot distinguish between the contribution of resonance states and the contribution of other states in the continuum to the photoemission cross section. Another important point is that when non-Hermitian quantum mechanics is applied we do not use the scalar product but instead should use the c product as discussed in refs 9 and 20. Let us briefly discuss the situation where we should not take the complex conjugate of the "bra" state when we calculate expectation values in non-Hermitian quantum mechanics and so-called left eigenstates are equal to the right eigenstates of the Floquet matrix. The QE states $|\Phi_k(t)\rangle$ are time-periodic

functions. We expand them in the Fourier basis set $f_n(t) \equiv \exp(i\omega nt)$, where $n = 0, \pm1, \pm2,...$ (i.e., $|\Phi_k(t)\rangle = \sum_n f_n(t)|\phi_{n,k}\rangle$). The Fourier components are spatial functions. They are the components of the right eigenvector of the Floquet Hamiltonian matrix

$$\mathscr{H}_{n',n} = 1/T\int_0^T \mathrm{d}t\,(f_{n'}(t))^*\left[-i\hbar\frac{\partial}{\partial t} + \hat{H}(\hat{\mathbf{r}}_j \exp(i\theta), t)\right]f_n(t) \quad (8)$$

Here, $\hat{\mathscr{H}}(\hat{\mathbf{r}}_j\exp(i\theta),t) = \hat{\mathscr{H}}_0$(complex-scaled) + $eF_0\exp(+i\theta)\sum_j \hat{z}_j\cos(\omega t)$. Note that in the calculation of the Floquet matrix elements we used the usual scalar product. From linear algebra, we know that the most general representation of a matrix is a complex and symmetric one. Therefore, without loss of generality, we consider the case where the Floquet matrix is equal to its transpose (i.e., $\mathscr{H}$ is a complex symmetric matrix). In such a case, the "left" eigenvectors of $\mathscr{H}$ are equal to the "right" eigenvectors. Therefore, we should *not* take the complex conjugate of the spatial Fourier components when we calculate expectation values. This means that the inner product is defined such that, for example, $(\phi_{n',k'}|\sum_j \hat{z}_j|\phi_{n,k}) = \langle\phi^*_{n',k'}|\sum_j \hat{z}_j|\phi_{n,k}\rangle$, where $\langle...\rangle$ stands for the usual definition of the scalar product. This inner product is known as the c product.[9] Consequently, the Floquet eigenstates are orthonormal functions under the definition

$$(1/T)\int_0^T \mathrm{d}t\langle\sum_{n'} f_{n'}(t)\,\phi^*_{n',k'}|\sum_n f_n(t)\,\phi_{n,k}\rangle = \delta_{k',k} \quad (9)$$

The time period is $T = {}^{2\pi}/_{\omega}$. In other words, we calculate the inner product as an integral over the spatial coordinates and over time where we do not take the complex conjugate of quantities that are complex merely because of complex scaling. This means that we conjugate the time-dependent functions f_n but not the spatial functions $\phi_{n,k}$. From eq 9, it follows that $\sum_n\langle\phi^*_{n,k'}|\phi_{n,k}\rangle = \delta_{k',k}$. Furthermore, when we take into account that states $|\Phi_k\rangle$ and $\exp(iN\omega t)|\Phi_k\rangle$ are orthogonal eigenstates of the Floquet operator for $N \neq 0$, we find that $\sum_n\langle\phi^*_{n+N,k}|\phi_{n,k}\rangle = \delta_{N,0}$ and finally $\langle\sum_{n'} f_{n'}(t)\,\phi^*_{n',k}|\sum_n f_n(t)\,\phi_{n,k}\rangle = 1$ for all times.

The probability of detecting an electron somewhere in space is equal to 1 at any given time because the number of particles in the entire space is conserved. However, high-energy photons are generated only because of the interaction of the electrons with the nuclei. Free electrons oscillating in the presence of the electromagnetic field do not emit high-energy photons. Therefore, the high harmonics are generated only within the lifetime of the resonance state. On the basis of this physical argument, we conclude that the number of electrons should not be conserved inside a finite box where the electrons interact with the nuclei. As time passes, the electrons escape from the finite box. Outside the box, we assume that the electron−nuclei interaction is equal to zero. The size of the box can be as large as one wishes. Within the framework of this box-quantization formalism, the number of electrons inside the box decays exponentially to zero as time passes. A similar approach has been taken before by Cederbaum and Tarantelli in their time-dependent formulation of the nuclear dynamics of decaying states.[21] The norm of the decaying wave packet is reduced in time because of the "loss" of electrons. We impose this time-dependent normalization on the quasi-energy resonance solutions by introducing the following complex phase factors: $\exp(-iE_{k_{res}}t/\hbar) = \exp(-i\mathscr{E}_{k_{res}}t/\hbar)\exp(-{}^1/_2\Gamma_{k_{res}}t/\hbar)$ for the "ket" Floquet states and $\exp(+iE^*_{k_{res}}t/\hbar) = \exp(+i\mathscr{E}_{k_{res}}t/\hbar)\exp(-{}^1/_2\Gamma_{k_{res}}t/\hbar)$ for the "bra" states. Thus, within the framework of the box quantization, we obtain for the state $|\Psi(t)\rangle = \exp(-iE_{k_{res}}t/\hbar)|\Phi_{k_{res}}(t)\rangle$ the normalization

$$(\Psi(t)|\Psi(t)) = \langle\exp(-iE_{k_{res}}t/\hbar)\sum_{n'} f_{n'}(t)\,\phi^*_{n',k_{res}}|\exp(-iE_{k_{res}}t/\hbar)\sum_n f_n(t)\,\phi_{n,k_{res}}\rangle = \exp(-\Gamma_{k_{res}}t/\hbar) \quad (10)$$

This means that the probability of detecting the system in a given atomic/molecular quasi-energy resonance (metastable) state decays exponentially in time with the decay rate $\Gamma_{k_{res}}$. To obtain this result, we used norm conservation for the states $|\Phi_{k_{res}}(t)\rangle$.

In conclusion, time-dependent expectation values are calculated as

$$(\Psi(t)|\,\hat{A}(t)|\Psi(t)) = \int\Psi^{\mathrm{L}}(\mathbf{r}_j, t)\,\hat{A}(t)\,\Psi^{\mathrm{R}}(\mathbf{r}_j, t)\prod \mathrm{d}^3r_j \quad (11)$$

where $\Psi^{\mathrm{R}}(\mathbf{r}_j, t) = \Psi(\mathbf{r}_j, t)$ and $\Psi^{\mathrm{L}}(\mathbf{r}_j, t)$ is obtained by taking the complex conjugate of $\Psi^{\mathrm{R}}(\mathbf{r}_j, t)$ except where quantities are complex merely because of the complex scaling of spatial coordinates.

Following our discussion, in non-Hermitian quantum mechanics, eq 6 is replaced by the following expression:

$$\sigma(\Omega) = |t_{\mathrm{res}}(\Omega) + t_{\mathrm{non-res}}(\Omega)|^2 \quad (12)$$

The resonance contribution to the photoemission cross section is given by

$$t_{\mathrm{res}}(\Omega) = \sum_{k'_{\mathrm{res}},k_{\mathrm{res}}} C^{\mathrm{L}}_{k'_{\mathrm{res}}}C^{\mathrm{R}}_{k_{\mathrm{res}}} \times \sum_{n=-\infty}^{+\infty}\sum_{n'=-\infty}^{+\infty} \frac{((E_{k_{\mathrm{res}}} - E^*_{k'_{\mathrm{res}}})/\hbar + \omega(n'-n))^2}{\Omega - [(E_{k_{\mathrm{res}}} - E^*_{k'_{\mathrm{res}}})/\hbar + \omega(n'-n)]}\langle\phi^*_{n',k'_{\mathrm{res}}}|\sum_j \hat{z}_j|\phi_{n,k_{\mathrm{res}}}\rangle \quad (13)$$

where the resonance Fourier components $\phi_{n,k_{\mathrm{res}}}$ are θ-dependent spatial functions, whereas the resonance complex quasi-energies are invariant with respect to θ.

An important point in the derivation of eq 13 is the time integration over $0 < t < \infty$. Physically, this is reasonable for laser pulses that are switched on at $t = 0$ and last longer than the lifetimes of the QE states. The correction for short pulses will be given below.

A more detailed derivation of eq 13 based on the time-independent scattering theory for time-dependent Hamiltonians[22,23] is beyond the scope of the present paper and will be given elsewhere.

To calculate the complex coefficients C^{R}_k and C^{L}_k in the expansions of the right and left wave functions

$$\Psi^{\mathrm{R}}_0(t=0) = \sum_{n,k} C^{\mathrm{R}}_k\phi_{n,k} \quad (14)$$

$$\Psi^{\mathrm{L}}_0(t=0) = \sum_{n,k} C^{\mathrm{L}}_k\,\phi_{n,k} \quad (15)$$

we should first explain how the complex-scaled initial state is obtained. Here we consider the general case in which the atom, before being exposed to the external laser field, is not in an eigenstate but in a linear combination of the field-free eigenstates. The unscaled initial wave packet is denoted $\Phi^{\mathrm{FF}}_0(\mathbf{r}_j)$. If

the field is suddenly turned on to its maximal field amplitude (the envelope of the laser field amplitude is a Heavyside function), then

$$C^{\mathrm{R}}_{k_{\mathrm{res}}} = \sum_n \langle \phi^*_{n,k_{\mathrm{res}}} | \Phi_0^{\mathrm{FF},\theta} \rangle \tag{16}$$

$$C^{\mathrm{L}}_{k_{\mathrm{res}}} = \sum_n \langle \Phi_0^{\mathrm{FF},-\theta} | \phi_{n,k} \rangle \tag{17}$$

where $\Phi_0^{\mathrm{FF},\theta}(\mathbf{r}_j) = \Phi_0^{\mathrm{FF}}(\mathbf{r}_j \exp(\mathrm{i}\theta))$. The other possibility is to turn the field on for several optical cycles. We choose this time equal to MT, where M is an integer and $T = {}^{2\pi}/_{\omega}$ is an optical cycle. The wave packet is propagated by solving the conventional time-dependent Schrödinger equation from $t = -MT$ to $t = 0$, yielding $\Phi_0(\mathbf{r}_j, t = 0)$, which is different from $\Phi_0^{\mathrm{FF}}(\mathbf{r}_j)$. The coefficients follow by projecting the complex-scaled wave function $\Phi_0^{\theta}(\mathbf{r}_j, t = 0)$ onto the complex QE Floquet solutions:

$$C^{\mathrm{R}}_{k_{\mathrm{res}}} = \sum_n \langle \phi^*_{n,k} | \Phi_0^{\theta}(t = 0) \rangle \tag{18}$$

$$C^{\mathrm{R}}_{k_{\mathrm{res}}} = \sum_n \langle \Phi_0^{-\theta}(t = 0) | \phi_{n,k} \rangle \tag{19}$$

If the laser is turned on adiabatically, then the coefficients are given by

$$C^{\mathrm{R}}_{k_{\mathrm{res}}} = C^{\mathrm{FF}}_{k_{\mathrm{res}}} \exp(-\mathrm{i}\int_{-MT}^{0} E^{\mathrm{ad}}_{k_{\mathrm{res}}}(t')\, \mathrm{d}t'/\hbar) \tag{20}$$

$$C^{\mathrm{L}}_{k_{\mathrm{res}}} = (C^{\mathrm{FF}}_{k_{\mathrm{res}}})^* \exp(+\mathrm{i}\int_{-MT}^{0} (E^{\mathrm{ad}}_{k_{\mathrm{res}}}(t'))^*\, \mathrm{d}t'/\hbar) \tag{21}$$

where the coefficients $C_{k_{\mathrm{res}}}{}^{\mathrm{FF}}$ are obtained by the projection of Φ_0^{FF} onto the field-free eigenstates and $E^{\mathrm{ad}}{}_{k_{\mathrm{res}}}$ are the adiabatic quasi-energies. Note that despite the adiabatic switching we assume that no relevant high harmonics are generated during the turn on. Clearly, this approach is valid only as long as there is no significant ionization during turn on (i.e., as long as the peak intensity is below the saturation intensity).

By substituting these coefficients into eq 13, we obtain the emission spectra. When the interference between different populated QE states is ignored, the double summation over k'_{res} and k_{res} in eq 13 is replaced by a single sum over k_{res}. Then, following the dynamical symmetry properties of the Floquet Hamiltonian for atoms, $\langle \phi^*{}_{n',k_{\mathrm{res}}} | \sum_j \hat{z}_j | \phi_{n,k_{\mathrm{res}}} \rangle = 0$ if $n' - n \neq 2m + 1$, where m is an integer (i.e., only odd harmonics are generated). The intensity of the high-order harmonic lines is then given by

$$\sigma(\Omega = (2m+1)\omega) \simeq \left| \sum_{k_{\mathrm{res}}} C^{\mathrm{L}}_{k_{\mathrm{res}}} C^{\mathrm{R}}_{k_{\mathrm{res}}} \frac{(\Omega - \mathrm{i}\Gamma_{k_{\mathrm{res}}}/\hbar)^2}{\Gamma_{k_{\mathrm{res}}}/\hbar} \times \sum_{n=-\infty}^{+\infty} \langle \phi^*{}_{n+2m+1,k_{\mathrm{res}}} | \sum_j \hat{z}_j | \phi_{n,k_{\mathrm{res}}} \rangle \right|^2 \tag{22}$$

Equation 22 suggests that the odd high-order harmonic generation spectrum is controlled by the narrowest populated QE resonance state. Let us explain this important result for the simple case where only one resonance QE state is populated (i.e., we have no summation over k_{res} in eq 22). In such a case, if $\hbar\Omega \gg \Gamma_{k_{\mathrm{res}}}$, then

$$\frac{(\Omega - \mathrm{i}\Gamma_{k_{\mathrm{res}}}/\hbar)^2}{\Gamma_{k_{\mathrm{res}}}/\hbar} \simeq \frac{\Omega^2}{\Gamma_{k_{\mathrm{res}}}/\hbar} \tag{23}$$

Consequently, the signal from state k_{res},

$$\sigma(\Omega = (2m+1)\omega) \approx \left(\frac{\Omega^2}{\Gamma_{k_{\mathrm{res}}}/\hbar} \right)^2 \left| \sum_{n=-\infty}^{+\infty} \langle \phi^*{}_{n+2m+1,k_{\mathrm{res}}} \left| \sum_j \hat{z}_j \right| \phi_{n,k_{\mathrm{res}}} \rangle \right|^2 \tag{24}$$

is proportional to $1/(\Gamma_{k_{\mathrm{res}}})$.[2] The assumption that only the narrowest (i.e, longest-lived) QE resonance state controls the photoinduced dynamics probably holds when one QE resonance state (usually associated with the field-free ground state) is narrower than all other resonance states by several orders of magnitude. Perhaps this is the reason that the experimental high-order harmonic generation spectra of helium fit so well with the results obtained from complex-scaling calculations[17] where it has been assumed that $\sigma(\Omega = (2m+1)\omega) \sim |\sum_{n=-\infty}^{\infty} \Omega^2 \langle \phi^*_{n+2m+1,k_0} | \sum_j \hat{z}_j | \phi_{n,k_0} \rangle|^2$, although the short high-intensity laser pulses used in the experiments should populate more than one QE state. However, one should be aware of the fact that the value of $\sigma(\Omega)$ when $\Omega = \omega(2m+1)$ does not only depend on the resonance width but also on the matrix elements $\langle \phi^*{}_{n+2m+1,k_{\mathrm{res}}} | \sum_j \hat{z}_j | \phi_{n,\, k_{\mathrm{res}}} \rangle$. Because of this dependence, although $\Gamma_{k_{\mathrm{res}}} < \Gamma_{k'_{\mathrm{res}}}$, the contribution of state k_{res} can be smaller than the contribution of state k'_{res}. This is possible when the difference between the resonance widths is not too large and when the two resonance wave functions have very different "lengths of localization" in Fourier space. Let us explain the last statement more carefully. The Fourier components satisfy the normalization condition $\sum_n \langle \phi^*{}_{n,k_{\mathrm{res}}} | \phi_{n,k_{\mathrm{res}}} \rangle = 1$. The localization length measures the number of dominant components in the Fourier expansion of the resonance QE Floquet complex-scaled wave function. By plotting the value of $\langle \phi^*{}_{n,k_{\mathrm{res}}} | \phi_{n,\, k_{\mathrm{res}}} \rangle$ versus n, the localization length in Fourier space can be obtained. It is clear that higher harmonic orders are obtained for QE resonance states with a longer localization length. We note in passing that QE states that are associated with classical chaotic dynamics are less localized in Fourier space than the QE states that are associated with a quasi-periodic regular classical photoinduced dynamics.[24] Without getting too deep into this subject, we can conclude that a QE state with a short lifetime may more efficiently generate high-order harmonics than another longer-lived resonance QE state, yet we still may expect that if a populated resonance QE state is narrower than the other resonances by several orders of magnitude then this narrow-resonance QE state will control the photoinduced dynamics.

So far we have discussed the HG spectra for cw lasers or for the case where the duration of the laser pulse supports many optical cycles, which justifies the use of Floquet theory. Before proceeding to the discussion of the conditions where sidebands are observable, let us generalize the derivation of eqs 22 and 24 to the cases where the laser pulses are very short. Using the (t, t') formalism, we find that the derivation of eq 5 and the expansion of $|\Phi_k\rangle$ also holds for nonperiodic time-dependent Hamiltonians.[25] In such a case, ω is not the cw laser frequency but is equal to $\omega = {}^{2\pi}/_{\tau}$ where τ is any finite time that is larger than the duration time of the pulse. However, when the dominant Fourier component of the laser pulse is the fundamental frequency of the laser, we may use the Floquet QE states as a basis set in our calculations of the time-dependent dipole moment, $d_{\mathrm{res}}(t)$. In such a case, ω in our expansion is the laser

frequency as before. However, the Fourier transform of $d_{res}(t)$ should be taken from 0 to τ_p rather than from 0 to ∞, where τ_p is the duration of the laser pulse. Therefore, when short laser pulses are applied, the term $1/\Gamma_{k_{res}}$ in eqs 22 and 24 should be replaced by $(1 - \exp(-\Gamma_{k_{res}}\tau_p/\hbar))/\Gamma_{k_{res}}$. For sufficiently short pulses, $(1 - \exp(-\Gamma_{k_{res}}\tau_p/\hbar))/\Gamma_{k_{res}} \simeq \tau_p/\hbar$. This shows that for ultrashort pulses the generation of high-order harmonics does not depend directly on the resonance width but rather on the matrix elements $\sum_{n=-\infty}^{+\infty}\langle\phi^*_{n+2m+1,\,k_{res}}|\sum_j \hat{z}_j|\phi_{n,k_{res}}\rangle$, which appear in eqs 22 and 24. Thus, when short laser pulses are applied, the resonance QE state making the dominant contribution to the HG spectrum will not necessarily be the longest-lived one. Clearly, in this case, the matrix elements must be evaluated for the system of interest in order to predict which QE states are dominant. In this respect, our general analysis is only the first step.

We return now to a discussion of the conditions that are required for the observation of sidebands (hyper-Raman lines). From eq 13, it follows that the hyper-Raman lines in the emission spectra are obtained at $\Omega = \mathcal{R}[(E_{k_{res}} - E^*_{k'_{res}})/\hbar] + \omega(n' - n) = (\epsilon_{k_{res}} - \epsilon_{k'_{res}})/\hbar + \omega(n' - n)$, where $n' - n = 2m + 1$ (i.e., odd values) or $n' - n = 2m$ (i.e., even values) and $k_{res} \neq k'_{res}$. The result of even or odd values of $n' - n$ depends on the dynamical symmetry properties of the complex-scaled QE resonance states as discussed above. Note that even orders are allowed when the parity symmetry of the two resonances is different. Here we proved that the hyper-Raman lines in the emission spectra are constructed of series of shifted odd and even high-order harmonics. The intensity of the hyper-Raman lines, resulting from the interference between two different resonance QE states $k_{res} \neq k'_{res}$, is given by

$$\sigma(\Omega = (\epsilon_{k_{res}} - \epsilon_{k'_{res}})/\hbar + N\omega) \simeq |C^L_{k'_{res}} C^R_{k'_{res}}|^2 \frac{\left[\Omega - \frac{i}{2\hbar}(\Gamma_{k_{res}} + \Gamma_{k'_{res}})\right]^2}{(\Gamma_{k_{res}} + \Gamma_{k'_{res}})/\hbar} \sum_{n=-\infty}^{+\infty} \left|\langle\phi^*_{n+N,k'_{res}}\left|\sum_j \hat{z}_j\right|\phi_{n,k_{res}}\rangle\right|^2 \quad (25)$$

We now apply the dynamical symmetry properties of the Floquet operator for atoms to eq 25. When the two QE states are degenerate eigenstates of the dynamical symmetry operator (even when they are nondegenerate eigenstates of the Floquet operator), the matrix elements vanish unless $N = 2m + 1$ with integer m. This means that the hyper-Raman lines are shifted odd harmonics. When the two QE states have different generalized parity (i.e., they are nondegenerate eigenstates of the dynamical symmetry operator), the matrix elements vanish unless $N = 2m$. If these two resonance QE states are degenerate eigenstates of the Floquet operator, even high-order harmonics will be obtained. If they are nondegenerate eigenstates of the Floquet operator, shifted even harmonics will be generated.

As one can see from eq 25, the intensity of the hyper-Raman lines in the emission spectra depends on the probability of populating two QE resonance states that can have different energies but should be associated with similar narrow widths.

This is a crucial point in our propositions for possible future experiments that should show the fingerprints of the hyper-Raman lines in the emission spectra: if $\Gamma_{k'_{res}} \gg \Gamma_{k_{res}}$, then the cross terms in eq 25 are negligible compared to the direct term in eq 22 that is associated with state k_{res}, and only odd harmonics will be observed. The hyper-Raman lines will be obtained only when $\Gamma_{k'_{res}} \approx \Gamma_{k_{res}}$.

As discussed above for the direct terms, the situation changes for very short pulses. Then, the harmonic intensities are not directly controlled by the widths of the resonance states. In this case, hyper-Raman lines may even be obtained when the populated QE states have significantly different lifetimes.

4. Illustrative Numerical Examples

In this section, we present numerical examples that corroborate the results of our discussion. These results are obtained by solving the time-dependent Schrödinger equation within the framework of conventional quantum mechanics. Hence, they serve as an independent check of the conclusions derived from non-Hermitian quantum mechanics. The Schrödinger equation is integrated numerically by means of the split-operator method[26] for laser-driven 1D model systems. In all cases, we employ trapezoidally shaped pulses where the field is switched on and off linearly. The HG spectra are calculated by taking the Fourier transform of the time-dependent dipole acceleration.[19] Here, the time integration is taken over the flat part of the pulse where the field amplitude is constant. First, we give two examples that demonstrate how the lifetimes determine the observability of the hyper-Raman lines. In another example, we show the effect of the laser pulse duration.

Our first example corresponds to typical HG experiments. We use an 800-nm laser pulse with an intensity of 1.5×10^{14} W/cm^2 and a model atom that reproduces the ionization potential of an Ar rare-gas atom (15.8 eV). The binding potential

$$V(x) = -\frac{e^2}{\sqrt{x^2 + 1.415}} \quad (26)$$

is a soft-core Coulomb potential. We consider (10−20−10) pulses (i.e., the duration of the constant-intensity part is 20 optical cycles, and the total pulse duration is 40 optical cycles). We consider three possibilities for the initial state of the system: (a) the field-free ground state $|\Phi_g\rangle$, (b) the field-free first excited state $|\Phi_e\rangle$, and (c) a superposition of the ground state and first excited state, $(|\Phi_g\rangle + |\Phi_e\rangle)/\sqrt{2}$. The two eigenstates have different parity (i.e., sidebands that may be generated from the interference between the two states are expected to be shifted even harmonics). The resulting HG spectra for the three cases are shown in Figure 1. The dashed lines mark the odd harmonic orders. We see that case a leads to an HG spectrum with only odd harmonics, as expected. In case b, the harmonic peaks are not as well defined because the first excited state is 8.8 eV higher in energy and therefore decays much faster than the ground state: the survival probabilities at the end of the pulse are 43% for the ground state and 2% for the excited state. The additional peaks in spectrum b indicate that more than one QE state is populated after the laser is turned on. Most interesting for us is case c, where we certainly have a superposition of several resonance QE states including the lowest-lying state that is associated with the field-free ground state. The interference between different QE states allows for the generation of sidebands. However, the sidebands are found only in a small part of the spectrum (orders below 20), and they are weaker than the odd harmonics. This agrees perfectly with our statement that the sidebands should be weak when the lifetimes of the interfering QE states differ greatly from each other.

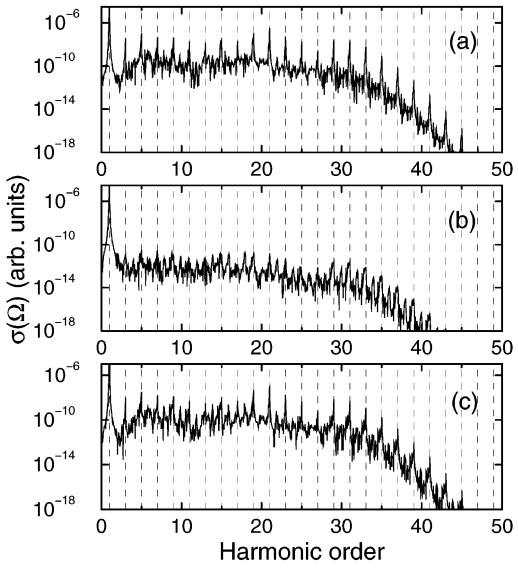

Figure 1. HG spectra for the Ar model atom in an 800-nm laser pulse with 1.5×10^{14} W/cm^2 intensity starting (a) from the ground state, (b) from the first excited state, and (c) from the superposition of the ground and first excited states.

In our second example, the conditions are made more favorable for the generation of sidebands. We employ an H_2^+ model potential

$$V(x) = -\frac{e^2}{\sqrt{\left(x-\frac{R}{2}\right)^2+2}} - \frac{e^2}{\sqrt{\left(x+\frac{R}{2}\right)^2+2}} \qquad (27)$$

with an internuclear distance of $R = 15$ au. The precise value of the soft-core parameter is not very important for our purposes. It is here set to 2, which reproduces the ionization potential of an isolated H atom (13.6 eV) for $R \rightarrow \infty$. The crucial difference to the model atom used in our first example is that, because of the large internuclear distance, the lowest two states are almost degenerate (8×10^{-4} eV difference). Therefore, these states have almost identical lifetimes. An 800-nm pulse with an intensity of 8×10^{13} W/cm^2 and a (10−20−10) envelope is used in the calculation. Again, we consider cases a−c as defined above. Figure 2 shows the resulting HG spectra. We find that both the ground state and the first excited state give a series of well-defined odd harmonics. Only in the cutoff region in panel a are some hyper-Raman lines found. The superposition state, however, gives a full series of hyper-Raman lines over the full range of the spectrum. In fact, the hyper-Raman lines are even-order harmonics. This agrees with our proof that the interference of degenerate QE states with different parity yields even harmonics.

In our third example, we demonstrate the effect of the laser pulse duration on the generation of hyper-Raman lines. In section 3, we have shown that for ultrashort pulses hyper-Raman lines may be generated even when the lifetimes of the populated QE states are very different. This happens when the pulse duration is shorter than the relevant lifetimes. We consider the model atom described by eq 26 in a 700-nm pulse with a relatively low intensity of 5×10^{13} W/cm^2. As a consequence, the lifetimes are much longer than in the first two examples. As the initial state, we take the superposition of the ground and first excited states. Figure 3 displays the HG spectra for two different pulse durations. The upper spectrum results from a (20−20−20) pulse, whereas the lower spectrum results from a

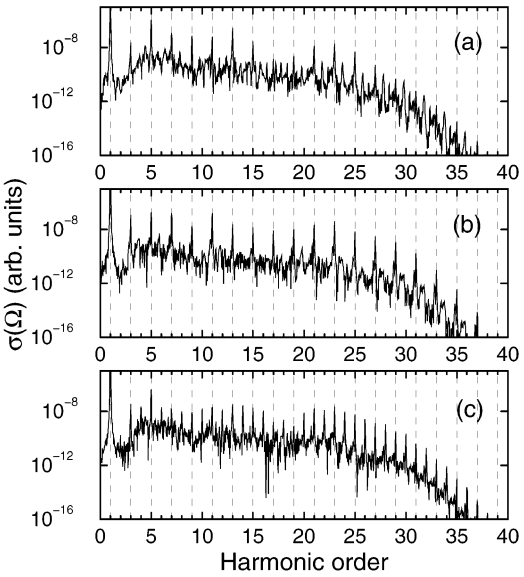

Figure 2. Same as Figure 1 for the H_2^+ model system at $R = 15$ au in an 800-nm pulse with an intensity of 8×10^{13} W/cm^2.

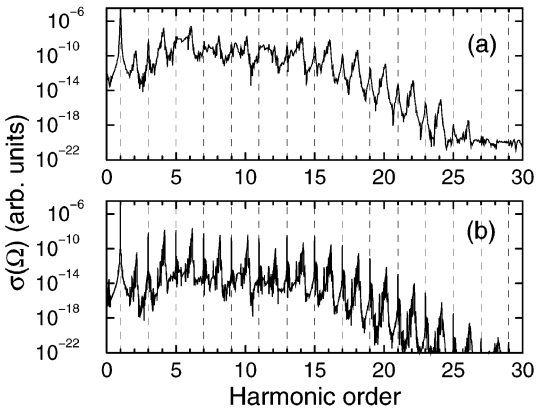

Figure 3. HG spectra for the Ar model atom in a 700-nm pulse with an intensity of 5×10^{13} W/cm^2 starting from a superposition of the ground and first excited states. (a) (20−20−20) pulse; (b) (20−160−20) pulse.

(20−160−20) pulse. The sidebands are present although the lifetimes of the ground and first excited states differ considerably. In the case of the shorter pulse, for example, the survival probabilities at the end of the pulse are 99 and 27%, respectively. Using the shorter pulse, the sidebands are stronger than the odd harmonics. By increasing the pulse duration, the odd harmonics become more dominant so that in the second spectrum the sidebands and the odd harmonics are equally important. Again, this shows that the odd harmonics generated by the longest-lived state become dominant for sufficiently long pulses. Furthermore, it is obvious that the odd harmonics are much sharper than the hyper-Raman lines as a consequence of the different lifetimes.

5. Proposition of Possible Experiments Revealing the Hyper-Raman Lines

Let us propose a scheme for an experiment where the hyper-Raman lines in the emission spectra will be shifted even high-order harmonic lines. We need to prepare as an initial state a linear combination of two QE narrow resonances with different parity but similar lifetimes (inverse widths). Let us discuss the possibilities of preparing such a situation in a one-electron atom.

It has been seen in previous numerical studies for the photoinduced dynamics of helium[17] that each one of the narrow quasienergy resonance states is dominated by a single ground or excited state of the field-free system. Therefore, it is also expected that the narrow QE states of the hydrogen atom are dominated by the ground state or one of the low excited states of the field-free atomic/molecular system. The QE state Φ_{1s}^{QE} that is dominated by the 1s hydrogen orbital is the longest-lived state. The QE state Φ_{2p}^{QE} that is dominated by the 2p hydrogen orbital is expected to have a shorter lifetime. If one prepares an initial state that equally populates the 1s and the 2p field-free hydrogen orbitals, then the sidebands may be observed, depending on the ratio between the two resonance widths. Following our discussion of eq 13, if Φ_{1s}^{QE} and Φ_{2p}^{QE} have very different resonance widths, then the sidebands will not be observable unless ultrashort pulses are used. The Φ_{2p}^{QE} and Φ_{2s}^{QE} states, however, are expected to have similar widths and thus similar lifetimes. Consequently, by preparing an initial state where the 2s and the 2p hydrogen levels are equally populated, the photoinduced dynamics of the hydrogen atom in a strong cw laser field will be controlled by the Φ_{2p}^{QE} and Φ_{2s}^{QE} states, and besides the odd harmonics, hyper-Raman lines should be observed.

Another example is helium. If the $\Phi^{QE}{}_{1s^2}$ and $\Phi^{QE}{}_{1s2p}$ states have similar widths, then sidebands in the HG spectra might be observed. If, however, these two resonance QE states are very different in their widths, then one should look for another linear combination of field-free states that may provide two QE states such that these are nondegenerate eigenfunctions of the dynamical symmetry operator and have similar resonance widths. Similar widths are expected for two states that are almost degenerate eigenstates of the complex-scaled Floquet operator. For example, such QE states can be Φ_{1s2s}^{QE} and $\Phi^{QE}{}_{1s2p}$. On the basis of our analysis, hyper-Raman lines are expected to be observed in the HG spectra by preparing the system in these two QE states.

To get a mixture of the two excited states, one should use one or two laser pulses with lower intensity to control the population of the two relevant states. Following Holthaus, one can use a single laser to control the population of two states by optimizing the shape and duration of the laser pulse.[27] Another possibility is to use the stimulated Raman adiabatic passage (STIRAP) scheme, which was proposed by Bergmann and coworkers.[14,28]

Acknowledgment. This paper is dedicated to Professor Don Kouri, a colleague and a friend, on his 65th birthday. He possesses that rare combination of genuine love for science and people, which is a model to follow. This work was supported in part by the US−Israel Binational Science Foundation, by the Basic Research Foundation administered by the Israeli Academy of Sciences and Humanities, and by the Fund for the Promotion of Research at the Technion. Dr. Ofir Alon is acknowledged for most enlightening discussions. N.M. thanks Professor Jan Michael Rost and the other members of the Finite Systems Division for many fruitful discussions and for their warm hospitality during the stay of N.M. at the Max Planck Institute for the Physics of Complex Systems in Dresden.

References and Notes

(1) Ferray, M.; L'Huillier, A.; Li, X. F.; Lompre, L. A.; Mainfray, G.; Manus, C. *J. Phys. B* **1988**, *21*, L31. Li, X. F.; L'Huillier, A.; Ferray, M.; Lompre, L. A.; Mainfray, G. *Phys. Rev. A* **1989**, *39*, 5751.

(2) See, for example, Protopapas, M.; Keitel, C. H.; Knight, P. L. *Rep. Prog. Phys.* **1997**, *60*, 389. Saliéres, P.; L'Huillier, A.; Antoine, P.; Lewenstein, M. *Adv. At., Mol., Opt. Phys.* **1999**, *41*, 83.

(3) Bartels, R.; Backus, S.; Zeek, E.; Misoguti, L.; Vdovin, G.; Christov, I. P.; Murnane, M. M.; Kapteyn, H. C. *Nature* **2000**, *406*, 164.

(4) Alon, O. E.; Averbukh, V.; Moiseyev, N. *Phys. Rev. Lett.* **2000**, *85*, 5218.

(5) Di Piazza, A.; Fiordilino, E. *Phys. Rev. A* **2001**, *64*, 013802.

(6) Bavli, R.; Metiu, H. *Phys. Rev. A* **1993**, *47*, 3299.

(7) Taylor, J. R. *Scattering Theory: The Quantum Theory of Nonrelativistic Collisions*; Wiley & Sons: New York, 1972.

(8) Reinhardt, W. P. *Annu. Rev. Phys. Chem.* **1982**, *33*, 223.

(9) Moiseyev, N. *Phys. Rep.* **1998**, *302*, 211.

(10) Ben-Tal, N.; Moiseyev, N.; Beswick, A. *J. Phys. B* **1993**, *26*, 3017.

(11) Alon, O. E.; Averbukh, V.; Moiseyev, N. *Phys. Rev. Lett.* **1998**, *80*, 3743.

(12) Moiseyev, N.; Chrysos, M.; Atabek, O.; Lefebvre, R. *J. Phys. B* **1995**, *28*, 2007.

(13) Kreibich, T.; Lein, M.; Engel, V.; U Gross, E. K. *Phys. Rev. Lett.* **2001**, *87*, 103901.

(14) Bergmann, K.; Shore, B. W. Coherent Population Transfer. In *Molecular Dynamics Spectroscopy by Stimulated Emission Pumping*; Dai, H. L., Field, R. W., Eds.; Advanced Series in Physical Chemistry; World Scientific: Singapore, 1995; Vol. 4, pp 315−373.

(15) Shirley, J. H. *Phys. Rev. B* **1975**, *138*, 979.

(16) Ben-Tal, N.; Moiseyev, N.; Kosloff, R.; Cerjan, C. *J. Phys. B* **1993**, *26*, 1445.

(17) Moiseyev, N.; Weinhold, F. *Phys. Rev. Lett.* **1997**, *78*, 2100.

(18) Corkum, P. B. *Phys. Rev. Lett.* **1993**, *71*, 1994.

(19) Burnett, K.; Reed, V. C.; Cooper, J.; Knight, P. L. *Phys. Rev. A* **1992**, *45*, 3347.

(20) *The Letropet Symposium View on a Generalized Inner Product*; Brändas, E.; Elander, N., Eds.; Lecture Notes in Physics; Springer: Berlin, 1987; Vol. 325.

(21) Cederbaum, L. S.; Tarantelli, F. *J. Chem. Phys.* **1993**, *98*, 9691.

(22) Peskin, U.; Moiseyev, N. *Phys. Rev. A* **1994**, *49*, 3712.

(23) Althorpe, S. C.; Kouri, D. J.; Hoffman, D. K.; Moiseyev, N. *Chem. Phys.* **1997**, *217*, 289.

(24) Averbukh, V.; Moiseyev, N.; Mirbach, B.; Korsch, H. J. *Z. Phys. D* **1995**, *35*, 247.

(25) Peskin, U.; Moiseyev, N. *J. Chem. Phys.* **1993**, *99*, 4590.

(26) Feit, M. D.; Fleck, J. A., Jr., Steiger, A. *J. Comput. Phys.* **1982**, *47*, 412.

(27) Holthaus, M. *Phys. Rev. Lett.* **1992**, *69*, 1596.

(28) Gaubatz, U.; Rudecki, P.; Schiemann, S.; Bergmann, K. *J. Chem. Phys.* **1990**, *92*, 5363.